# Balance of corneal horizontal coma by internal optics in eyes with intraocular artificial lenses: Evidence of a passive mechanism

Susana Marcos    , Patricia Rosales , Lourdes Llorente , Sergio Barbero ,
I. Jiménez-Alfaro [a,b]

*Instituto de Óptica "Daza de Valdés", Consejo Superior de Investigaciones Científicas, Madrid, Spain*
*Fundación Jiménez Díaz, Madrid, Spain*

## Abstract

It is well known that the aberrations of the cornea are partially compensated by the aberrations of the internal optics of the eye (primarily the crystalline lens) in young subjects. This effect has been found not only for the spherical aberration, but also for horizontal coma. It has been debated whether the compensation of horizontal coma is the result of passive mechanism [Artal, P., Benito, A., & Tabernero, J. (2006). The human eye is an example of robust optical design. *Journal of Vision, 6* (1), 1–7] or through an active developmental feedback process [Kelly, J. E., Mihashi, T., & Howland, H. C. (2004). Compensation of corneal horizontal/vertical astigmatism, lateral coma, and spherical aberration by internal optics of the eye. *Journal of Vision, 4* (4), 262–271]. In this study we investigate the active or passive nature of the horizontal coma compensation using eyes with artificial lenses, where no active developmental process can be present. We measured total and corneal aberrations, and lens tilt and decentration in a group of 38 eyes implanted with two types of intraocular lenses designed to compensate the corneal spherical aberration of the average population. We found that spherical aberration was compensated by 66%, and horizontal coma by 87% on average. The spherical aberration is not compensated at an individual level, but horizontal coma is compensated individually (coefficients of correlation corneal/internal aberration: −0.946, $p < 0.0001$). The fact that corneal (but not total) horizontal coma is highly correlated with angle lamda (computed from the shift of the 1st Purkinje image from the pupil center, for foveal fixation) indicates that the compensation arises primarily from the geometrical configuration of the eye (which generates horizontal coma of opposite signs in the cornea and internal optics). The amount and direction of tilts and misalignments of the lens are comparable to those found in young eyes, and on average tend to compensate (rather than increase) horizontal coma. Computer simulations using customized model eyes and different designs of intraocular lenses show that, while not all designs produce a compensation of horizontal coma, a wide range of aspheric biconvex designs may produce comparable compensation to that found in young eyes with crystalline lenses, over a relatively large field of view. These findings suggest that the lens shape, gradient index or foveal location do not need to be fine-tuned to achieve a compensation of horizontal coma. Our results cannot exclude a fine-tuning for the orientation of the crystalline lens, since cataract surgery seems to preserve the position of the capsule.

*Keywords:* Ocular aberrations; Compensation; Cornea; Crystalline lens; Intraocular lens; Misalignment

## 1. Introduction

The relative contribution of the cornea and crystalline lens to the overall ocular wave aberration is a relevant question in both the basic study of human eye optical quality and clinical ophthalmic applications. It is known that there are differences in the aberrations of the ocular components and their interactions between different refractive groups (myopic, emmetropic and hyperopic eyes) due to the different geometrical properties of these eyes (Artal, Benito, & Tabernero, 2006; Coletta, Han, & Moskowitz, 2006; Llorente, Barbero, Cano, Dorronsoro, & Marcos,

2004) as well as the fact that the structural properties of the crystalline lens (Dubbelman & Heijde, 2001; Glasser & Campbell, 1998), and the cornea to a lesser extent (Dubbelman, Sicarn, & Van der Heijde, 2006) change over time, leading to a significant increase of the aberrations with age (Applegate, Donnelly, Marsack, Koenig, & Pesudovs, 2007; Artal, Berrio, Guirao, & Piers, 2002; Calver, Cox, & Elliott, 1999; Mclellan, Marcos, & Burns, 2001). On the other hand, refractive and intraocular corrections change the natural structure of the ocular components: corrections with contact lenses (particularly rigid gas permeable) alter the relative contribution of the ocular components to retinal image quality and individual interactions of aberrations play a role on their optical performance (Dorronsoro, Barbero, Llorente, & Marcos, 2003); corneal refractive surgery modifies corneal shape and therefore corneal aberrations (Applegate & Howland, 1997; Marcos, Barbero, Llorente, & Merayo-Lloves, 2001); and in cataract surgery the crystalline lens is replaced by intraocular lenses which specific design (spherical or aspheric), in combination with the optics of the other components of the eye (cornea), determines the final optical quality of the eye (Barbero, Marcos, & Jimenez-Alfaro, 2003; Marcos, Barbero, & Jiménez-Alfaro, 2005).

Although the magnitude and distribution of ocular aberrations differ substantially across subjects, a balance of corneal aberrations by internal optics, resulting in smaller ocular aberrations than those of the individual ocular components appears to be a common trend in young eyes. Several studies have shown that the spherical aberration of the cornea is generally positive, while that of the crystalline lens is negative, reducing the total spherical aberration of the eye (Artal & Guirao, 1998; Barbero, Marcos, & Merayo-Lloves, 2002; El Hage & Berny, 1973; Glasser & Campbell, 1999; Sivak & Kreuzer, 1983; Smith & al, 2001; Tomlinson, Hemenger, & Garriott, 1993). More recent studies have also shown a reduction of corneal third-order coma by internal optics in young eyes (Artal, Guirao, Berrio, & Williams, 2001; Coletta et al., 2006; Kelly, Mihashi, & Howland, 2004). The contribution of the posterior surface of the cornea to this compensation seems to be practically negligible (Dubbelman, Sicam, & van der Heijde, 2007) and therefore the crystalline lens appears to be the major responsible of the effect. This corneal/internal balance of spherical aberration and coma has been shown to get disrupted in older eyes (Artal et al., 2002), presumably because of structural changes in the crystalline lens, producing the reported increase of aberrations with age.

The question whether the corneal/internal compensation arises from a passive mechanism or through an active developmental feedback process has been debated. Similarly to the emmetropization process that leads ocular growth to emmetropia by actively adjusting eye length to the optical power of the cornea and crystalline lens, it has been suggested that high order aberrations may equally "emmetropize", by tuning the geometry of the ocular surfaces, gradient index distribution or position to achieve optimal image quality. A cross-sectional study in humans from age 5 (Brunette, Bueno, Parent, Hamam, & Simonet, 2003) and longitudinal studies in animal models (García de la Cera, Rodriguez, & Marcos, 2006; Kisilak, Campbell, Hunter, Irving, & Huang, 2006) show a decrease of aberrations during development. While it has been suggested that visual feedback cannot be excluded from playing a role in an active compensation of aberrations (Kisilak et al., 2006), a decrease of aberrations (coma in particular) occurs in chicks during the first two weeks post-hatching, even in eyes occluded with diffusers, and therefore with no visual feedback (García de la Cera et al., 2006), suggesting a passive mechanism. In fact, a simple geometrical model of the growing chick eye can predict an improvement of optical quality with age, for a constant pupil size (Howland, 2005).

Kelly and colleagues (Kelly et al., 2004) in a study involving 30 normal young human eyes, found a significant average corneal/internal compensation of horizontal/vertical astigmatism, spherical aberration and horizontal coma. Individually, they did not find a significant correlation between corneal and internal spherical aberration, what led them to suggest that the average compensation of spherical aberration observed was inherent to the geometrical properties of the cornea and the lens and was probably determined over the course of evolution (i.e. due to a passive mechanism). For horizontal coma, however, they found that the compensation occurred individually and suggested an active fine-tuning between the cornea and crystalline lens (i.e. by subtle tilting or decentering of the lens) that would reduce horizontal coma during development.

Artal and collegues (Artal et al., 2006) investigated specifically the compensation of horizontal coma in a group of 73 myopic and hyperopic young eyes. They found that, while corneal horizontal coma typically was larger in hyperopic eyes (showing larger displacements of the pupil center with respect to the corneal reflex), compensation occurred equally in both groups, resulting in similar amounts of ocular horizontal coma. They concluded that compensation resulted from the geometrical structure of the eye, and was primarily a passive mechanism.

The active or passive nature of the compensation mechanism can be investigated using eyes with artificial lenses, which cannot be subject to an active developmental process. We investigated the compensation of horizontal coma in a group of patients that had undergone cataract surgery, with replacement of the crystalline lens by intraocular lenses (IOLs). The IOLs were of two different types, with aspheric anterior and posterior surfaces, respectively, producing negative internal spherical aberration, aiming at compensating the average spherical aberration of the cornea. The comparison of the compensation of horizontal coma in these eyes with that reported in previous studies in normal eyes will shed light into the nature of the compensation mechanism.

## 2. Methods

### 2.1. Subjects

A total of 38 eyes from 21 patients participated in the study. All patients had undergone uneventful cataract surgery (phacoemulsification with 3.2-mm superior clear corneal incision) at least 2 months before the measurements. In all cases, the implanted IOLs had an aspheric design producing negative internal spherical aberration. The IOLs were either Tecnis (Advanced Medical Optics), with aspheric anterior surface (Group 1, $n = 18$) or Acrysof IQ (Alcon Research Laboratories), with aspheric posterior surface (Group 2, $n = 20$). Table 1 summarizes the profile of the eyes of the study. The experimental protocols were approved by Institutional Review Boards and met the Declaration of Helsinki. All subjects signed an Informed Consent Form after the nature of the study and potential consequences had been explained.

### 2.2. Corneal aberrations

The anterior corneal elevation was obtained using a Placido disk videokeratoscope (Humphrey-Zeiss MasterVue Atlas), for a 10-mm area centered at the corneal reflex. Corneal elevations were exported as a grid sag surface to a computer eye model programmed in an optical design software (Zemax). Corneal aberrations were computed assuming a spherical posterior corneal surface of 6.5 mm radius, a corneal refractive index of 1.376, and a wavelength of 786 nm. Computations were done referred to the pupil center, and accounting for the misalignment between the videokeratoscopic axis and the line of sight, i.e, with a field angle for incoming rays accounted for by the displacement of the 1st Purkinje image with respect to the pupil center, assuming a center of rotation 15 mm behind the cornea. As a control, corneal aberrations were also computed assuming a lateral shift of the reference, rather than a rotation. Corneal wave aberrations were obtained for the maximum pupil diameter available in total wave aberrations in the same patients. Corneal wave aberrations were fit to 7th order Zernike polynomials, and the OSA standards for reporting aberrations were followed. Third order horizontal coma ($Z_3^1$) and 4th order spherical aberration ($Z_4^0$) were reported.

Pre- and post-operative anterior corneal aberrations had already been reported on this group of eyes (part of a larger sample of 43 eyes), that had participated in a study on incision-induced corneal aberrations (Marcos, Rosales, Llorente, & Jimenez-Alfaro, 2007). The corneal aberrations previously reported differ on those reported here in several aspects: they had been calculated using the corneal reflex as a reference and they referred to anterior corneal aberrations assuming no posterior corneal surface, and a refractive index of 1.3367.

### 2.3. Total aberrations measurements

Total wave aberrations were measured using a second generation laser ray tracing (LRT), which was developed at the Instituto de Óptica (CSIC) in Madrid, Spain (Llorente et al., 2004). In this technique, described and validated in detail in previous publications (Llorente, Diaz-Santana, Lara-Saucedo, & Marcos, 2003; Marcos, Díaz-Santana, Llorente, & Dainty, 2002; Moreno-Barriuso, Marcos, Navarro, & Burns, 2001) a scanning system scans a narrow 786-nm laser beam across the pupil. Ray aberrations are obtained by estimating the deviations of the centroids of the retinal spots images corresponding to each entry pupil location with respect to the reference (chief ray). These deviations are proportional to the local derivatives of the wave aberrations. Measurements were done under mydriasis (1 drop 1% tropicamide). Pupil diameters ranged from 4 to 6 mm, and the sampling pattern (with 37 samples in a hexagonal configuration) was adjusted by software to fit the natural pupil. Spherical error was corrected by means of a Badal focusing system. Total wave aberrations were fit to 7th order Zernike polynomials, and the OSA standards for reporting aberrations (Applegate et al., 2000) were followed. Third order horizontal coma $Z_3^1$ and 4th order spherical aberration $Z_4^0$ were reported.

Internal aberrations were obtained by subtraction of total minus corneal aberrations.

### 2.4. Angle λ, IOL tilt and decentration

IOL tilt and decentration were measured with a custom developed Purkinje imaging system described and experimentally validated elsewhere (de Castro, Rosales, & Marcos, 2007; Rosales & Marcos, 2006, 2007). In brief, in this method images of PI, PIII and PIV (first, third and fourth Purkinje Images) are obtained with eccentric (14 deg) collimated illumination from LEDs and captured on an IR CCD camera provided with a telecentric lens. The method to obtain tilt and decentration from the relative locations of PI, PIII and PIV assumes a linear relation between Purkinje image positions and rotation of the eye ($\beta$), lens tilt ($\alpha$) and lens decentration ($d$) (Barry, Dunne, & Kirschkamp, 2001; Phillips, Perez-Emmanuelli, Rosskothen, & Koester, 1988). Coefficients in the set of linear equations are obtained using eye modelling in Zemax. IOL tilt is referred to the pupillary axis and the IOL decentration ($d$) is referred to the pupil center. Sign conventions for the horizontal components (tilt around y and horizontal decentration), which are those relevant to this study are: positive tilt means that the nasal edge of the lens moves backward (right eyes) or forward (for the left eye), and viceversa for negative. Positive decentration means that the lens is shifted toward the nasal (right eye) or temporal (left eye) direction and viceversa for negative.

The Purkinje imaging system was also used to estimate the relative shift of the corneal reflex (first Purkinje image) with respect to the pupil center for foveal fixation, and angle $\lambda$ was calculated as described elsewhere (Rosales & Marcos, 2007). Sign conventions for the horizontal component are: positive, the line of sight rotates to the nasal (right eye) or temporal side (left eye) of the pupillary axis and viceversa for negative.

Additionally, the Purkinje imaging system has a channel for phakometry measurements (Rosales, Dubbelman, Marcos, & van der Heijde 2006; Rosales & Marcos, 2006).

Measurements of lens tilt and decentration were obtained in dilated eyes, in the same session as total and ocular aberrations. This guaranteed that measurements were not affected by potential changes of pupil center with pupil size. Optical biometry (with the IOLMaster, Zeiss) was obtained in all eyes, and phakometry (with the phakometry mode of the Purkinje imaging apparatus) was performed when the radii of curvature of the IOL were not known, since those parameters are required to process the data. A full description of the technique, experimental procedure and schematic diagrams to illustrate the sign conventions can be found in previous publications (de Castro et al., 2007; Rosales & Marcos, 2006, 2007; Rosales, Wendt, Marcos, & Glasser, 2007).

Lens tilt and decentrations had already been reported in a subset of 21 eyes (12 patients) who participated in a study comparing IOL tilt and decentration from Scheimpflug and Purkinje imaging (de Castro et al., 2007)

### 2.5. Computer eye modelling

Customized computer eye models in Zemax were used to compare predictions of horizontal coma (with and without IOL lens tilt and decentration) with real measurements. Simulations were performed for 15 eyes

#### Table 1
Eyes' profile

|  | Group 1 ($n = 18$) | Group 2 ($n = 20$) |
| --- | --- | --- |
| Age (yr) | $63.77 \pm 15.20$ | $72.07 \pm 3.27$ |
| # Males/# females | 13/7 | 12/6 |
| # Patients/# eyes | 11/20 | 10/18 |
| # OD/# OS | 11/9 | 9/9 |
| Pre-operative | $-1.75 \pm 3.21$ | $-1.41 \pm 2.66$ |
| *Spherical error (D)* |  |  |
| Axial length | $23.28 \pm 0.89$ | $23.20 \pm 0.87$ |
| IOL power (D) | $21.15 \pm 3.75$ | $20.60 \pm 2.02$ |

from Group 2, for which a full geometrical description was available. A full description of the customized computer eye has been presented elsewhere (Rosales & Marcos, 2007).

### 2.6. Data analysis

Right and left eyes were included in the study, to test for mirror symmetry, and in view of the fact that surgeries were carried out independently. For average calculations, the sign of horizontal coma was reversed in right eyes (Kelly et al., 2004; Marcos & Burns, 2000; Smolek, Klyce, & Sarver, 2002) to account for the enantiomorphism of the right and left eyes. Otherwise, data from left and right eyes are presented without changing signs. The individual compensation of corneal by internal aberrations (spherical aberration and horizontal coma) was tested by means of correlations. Relationships between total and corneal horizontal coma and angle $\lambda$, and between angle $\lambda$ and IOL tilt and decentration (horizontal components) were tested using linear regressions.

Statistical analysis was performed using Matlab: unpaired two-tailed $t$-tests were used to test the statistical significance of mean differences across Groups 1 and 2; a Wilcoxon signed rank test was used to test the statistical significance of differences across mean total and corneal aberrations (to assess the compensatory role of the internal optics); and a $z$-test was used to test the statistical significance of correlations. Statistical significance was set to the $p < 0.01$ level for all tests.

Finally, both for averages and correlation analysis, corneal and total aberration data were scaled from the maximum pupil diameter down to 5-mm. Therefore 6 patients from Group 1 and 5 patients from Group 2 with pupil diameters smaller than 5 mm were excluded for this analysis. Angle $\lambda$ was available from all eyes, whereas IOL tilt and decentration was missing in 3 eyes from Group 1 and 5 eyes from Group 2 (where the third Purkinje image was vignetted by the pupil).

## 3. Results

### 3.1. Average compensation

We investigated the compensation of spherical aberration and horizontal coma on the entire sample, and Groups 1 and 2 separately. The mean coefficient values are shown in Table 2, for 5-mm pupils (eyes with pupils smaller than 5-mm pupils were not included).

These results are indicative of a high compensation of the corneal spherical aberration of the average population, in keeping with the intended performance of the aspheric IOL designs. The compensation of the corneal horizontal coma is also highly statistically significant, with average

reduction close to 90%. Compensation is slightly higher for Group 1 than 2, although the resulting total aberration is not statistically significantly different across groups.

### 3.2. Individual compensation

Individually, 16 eyes from 18 in Group 1 and 18 eyes from 20 in Group 2 showed a reduction of corneal spherical aberration. In two eyes, with almost zero or negative corneal spherical aberration there was a shift of the spherical aberration toward negative values (with a larger absolute total than corneal aberration). In 11 eyes from 18 in Group 1 and 20 eyes from 20 in Group 2 there is a reduction of the absolute value of horizontal coma. In 4 eyes from Group 1 there is an overcompensation of horizontal coma, which resulted in larger absolute total than corneal aberration.

Quantitative analysis of compensation of spherical aberration and horizontal coma on an individual basis was performed by testing for linear correlations between internal and corneal values for these aberrations. Fig. 1 shows internal versus corneal spherical aberration, for 5-mm pupils (only eyes with pupil diameters of 5-mm and larger are therefore included). In most eyes, internal spherical aberration is negative. Although the IOLs are nominally designed to exhibit a constant negative spherical aberration (for a specific model eye), there is a significant scattering in the internal spherical aberration. These differences arise from the fact that estimates of internal aberrations incorporate the effect of ray convergence from the cornea, and therefore they are affected by corneal curvature and anterior chamber depth, which differ across subjects. These individual differences in internal aberrations are predicted by customized model eyes that introduce individual ocular biometry (Rosales & Marcos, 2007). There is no significant correlation between corneal and internal spherical aberration values, confirming that compensation is not provided at an individual level. Fig. 2 shows a significant linear negative correlation ($p = 0.0035$) between corneal and internal horizontal coma, for 5-mm pupils. The sign of horizontal coma has not been reversed for right eyes (closed symbols). Table 3 shows correlation coefficients, $p$ values and slopes

Table 2
Average values of spherical aberration and horizontal coma, for 5-mm pupils

| | Total | Corneal | % Compensation | $p$ value[a] |
|---|---|---|---|---|
| *Spherical aberration $Z_4^0$ ($\mu m$)* | | | | |
| Group 1 | 0.035 ± 0.07 | 0.13 ± 0.06 | 73.6 | <0.0001* |
| Group 2 | 0.041 ± 0.06 | 0.096 ± 0.06 | 57.0 | <0.0001* |
| All eyes | 0.038 ± 0.06 | 0.11 ± 0.06 | 66.2 | <0.0001* |
| $p$ value[b] | 0.79 | 0.13 | | |
| *Horizontal coma $Z_3^1$ ($\mu m$)* | | | | |
| Group 1 | 0.005 ± 0.10 | 0.11 ± 0.12 | 94.8 | 0.0068* |
| Group 2 | 0.038 ± 0.05 | 0.24 ± 0.19 | 84.3 | <0.0001* |
| All eyes | 0.023 ± 0.08 | 0.18 ± 0.17 | 87.3 | <0.0001* |
| $p$ value[b] | 0.30 | 0.033 | | |

Group 1, $n = 12$; Group 2, $n = 15$; All eyes, $n = 27$.
(a) $p$-value, indicating significant compensation (*), for Wilcoxon signed rank test (b) $p$-value, indicating significant differences across groups (*), for unpaired two-tailed $t$-test.
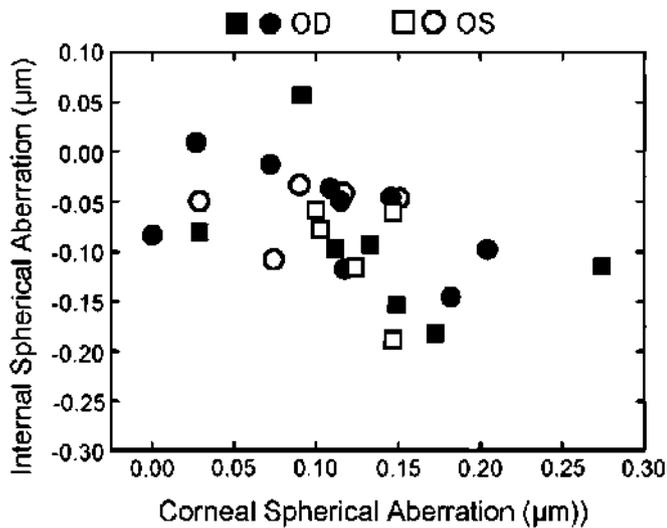
Fig. 1. Corneal spherical aberration versus internal spherical aberration. Closed symbols stand for right eyes, and open symbols for left eyes. Circles stand for eyes from Group 1 (anterior surface asphericity IOLs) and squares for eyes from Group 2 (posterior surface asphericity IOLs). Data are for 5-mm pupil diameters.
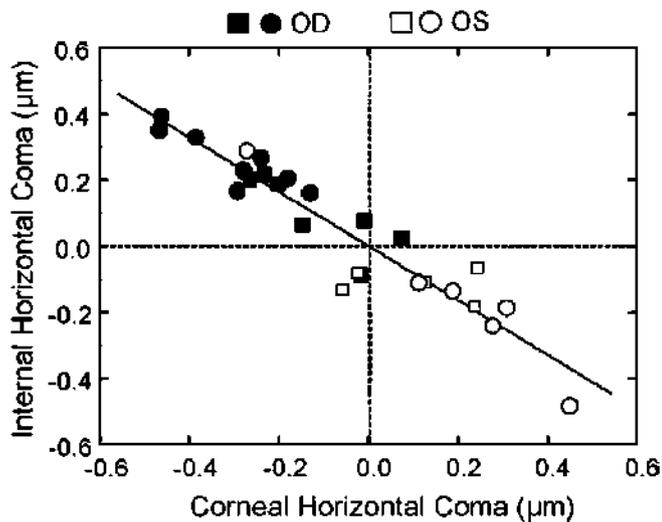


Fig. 2. Corneal horizontal coma versus internal horizontal coma, showing a significant linear correlation ($r = -0.946$, $p < 0.0001$). Closed symbols stand for right eyes, and open symbols for left eyes. Circles stand for eyes from Group 1 (anterior surface asphericity IOLs) and squares for eyes from Group 2 (posterior surface asphericity IOLs). Data are for 5-mm pupil diameters.

for each group and all eyes together for spherical aberration and horizontal coma.

A perfect compensation occurs for a slope of $-1$. No significant correlations were found for spherical aberration, but we found significant correlations for horizontal coma, with slopes of $-0.82$.

### 3.3. Effect of angle $\lambda$

Fig. 3 shows the shift of the Purkinje image (horizontal and vertical coordinates) with respect to the pupil center

Table 3
Correlations, significance and slopes of the linear regression of corneal and internal coefficients, for spherical aberration and horizontal coma

| | Coefficient of correlation $R$ | $p$ | Slope |
|---|---|---|---|
| Corneal vs Internal Spherical Aberration $Z_4^0$ (μm) | | | |
| Group 1 | -0.418 | 0.176 | -0.418 |
| Group 2 | -0.258 | 0.395 | -0.169 |
| All eyes | -0.423 | 0.035 | -0.347 |
| Corneal vs Internal Horizontal coma $Z_3^1$ (μm) | | | |
| Group 1 | -0.799 | 0.001* | -0.662 |
| Group 2 | -0.979 | <0.0001* | -0.852 |
| All eyes | -0.946 | <0.0001* | -0.819 |

Group 1, $n = 12$; Group 2, $n = 15$; All eyes, $n = 27$.

measured in all eyes of the study (circles and squares). On the same plot we have superimposed (broken circles and squares) the estimated angle of rotation of the model eye (customized to each patient) needed to achieve the measured 1st Purkinje image shift (related to angle $\lambda$). As expected, there is mirror left/right eye symmetry in the horizontal coordinates of Purkinje shift and angle $\lambda$. There are significant differences ($p < 0.0001$, unpaired $t$-test) in the mean horizontal 1st Purkinje shift (or angle $\lambda$) between Groups 1 and 2 (0.17 mm or 1.34 deg, and 0.43 mm or 3.52 deg, on average, respectively), which explains the marginally significant difference in corneal horizontal coma (Table 2).

Individually, there are highly significant correlations between corneal horizontal coma and the horizontal component of angle $\lambda$ (Fig. 4, open and filled circles), indicating that corneal horizontal coma arises primarily from the misalignment of the pupillary axis and the line of sight. For total horizontal coma there is a slight dependency with $\lambda$ in the same direction of corneal coma (Fig. 4, open and filled squares). Table 4 shows coefficients of correlation coefficients, $p$ values and slopes for each group and all eyes together, for the linear regressions of corneal and total horizontal coma as a function of angle $\lambda$.

### 3.4. Effect of IOL tilt and decentration

IOL tilt (measured with respect of the pupillary axis) and IOL decentration (with respect to the pupil center) also exhibit left/right eye midline symmetry, as shown in Fig. 5A (horizontal vs vertical coordinates of IOL tilt) and Fig. 5B (horizontal vs vertical coordinates of IOL decentration), as had been reported previously for the crystalline lens (Rosales & Marcos, 2006). On average, IOLs are tilted by $+1.86 \pm 1.29$ deg for Group 1 and $+1.35 \pm 0.74$ deg for Group 2, with no statistically significant differences between the two groups ($p = 0.20$) and decentered nasally by 0.25 mm for Group 1 and 0.29 mm for Group 2, with no statistically significant differences between the two groups ($p = 0.20$).

We made use of a customized model eye (Rosales & Marcos, 2007) to test whether IOL tilt and decentration
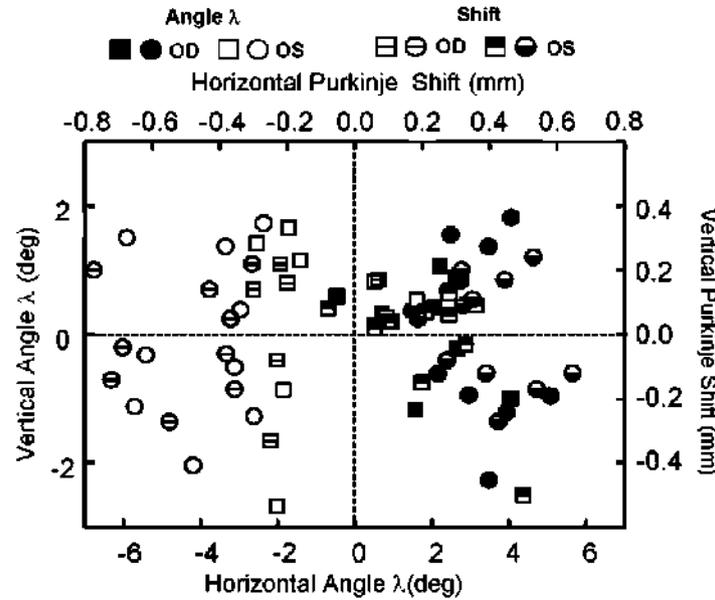
Fig. 3. Horizontal and vertical shift of the 1st Purkinje image with respect to the pupil center (top horizontal and right vertical axes, respectively), and the equivalent horizontal and vertical coordinates of angle $\lambda$ (bottom horizontal and left vertical axes, respectively, and broken symbols), for the eyes of the study. Closed symbols stand for right eyes, and open symbols for left eyes. Circles stand for eyes from Group 1 (anterior surface asphericity IOLs) and squares for eyes from Group 2 (posterior surface asphericity IOLs). Sign conventions for the 1st Purkinje image shift with respect of the pupil center are as follows. For horizontal shift x: Positive, the Purkinje image is shifted toward the nasal direction and viceversa for negative. For vertical shift: Sign conventions are: Positive, the Purkinje image is shifted upward and viceversa for negative. Sign conventions for angle $\lambda$ are as follows. For the horizontal coordinate: Positive, the line of sight is rotated upwards with respect to the pupillary axis. Negative, the line of sight is rotating downwards referred to the pupillary axis. For the vertical coordinate: Positive, the line of sight is rotated to the nasal (right eye) or temporal side (left eye) and viceversa for the Negative.
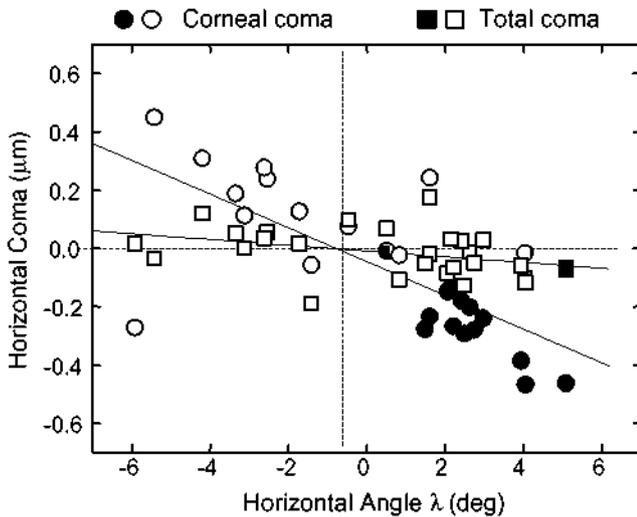


Fig. 4. Horizontal coma as a function of angle $\lambda$ (see Fig. 3). Data from Groups 1 and 2 have been combined. Circles stand for corneal coma and squares for total coma. Closed symbols represent right eyes and open symbols left eyes. Solid lines represent linear correlations to the data ($r = -0.71$, $p < 0.0001$, for corneal, and $r = -0.36$, $p = 0.058$ for total). Data are for 5-mm pupil diameters.

induced additional coma, or on the contrary played a compensatory role. Wave aberrations were estimated, assuming no tilt and decentration of the IOL, i.e. collinear with the pupillary axis, and also introducing the measured amounts of tilt and decentration. Internal aberrations were com-

puted for each condition, subtracting total minus corneal aberrations. Fig. 6 presents linear correlations of internal vs corneal horizontal coma, with data from the simulations assuming a centered lens in circles, with the actual tilt and decentration in triangles, and the experimental data in squares. Results are for 15 eyes from Group 2. The slope of the correlation of corneal versus simulated internal horizontal coma increases from $-0.62$ to $-0.96$ (gets closer to 1) when IOL tilt and decentration are incorporated, revealing that IOL tilt and decentration contribute to the compensation of horizontal coma. Predicted values are close to the experimental values of horizontal coma (particularly for right eyes shown in the left side of the graph). The slope of the corneal vs real total horizontal coma in this group of eyes is $-0.81$. In all three cases, the coefficient of correlation is higher than $-0.958$ and $p < 0.0001$.

## 4. Discussion

We found a systematic compensation of corneal horizontal coma in eyes implanted with artificial lenses, designed to correct for the corneal spherical aberration of the average population. The compensation of spherical aberration over a sample-wide population (66.2%) is of the same order or even larger than that found in young eyes with natural crystalline lenses. For example, previous studies found an average compensation of spherical aberration of 52% ($n = 7$, (Artal et al., 2001)), or 36% ($n = 30$, (Kelly

Table 4
Correlations, significance and slopes of the linear regression of corneal and total horizontal coma as a function of angle $\lambda$

| | Coefficient of correlation $R$ | $p$ | Slope ($\mu$m/deg) |
|---|---|---|---|
| *Corneal horizontal coma vs angle $\lambda$* | | | |
| Group 1 ($n = 12$) | −0.5464 | 0.0534 | −0.0504 |
| Group 2 ($n = 15$) | −0.7965 | 0.0004* | −0.0843 |
| All eyes ($n = 27$) | −0.7105 | <0.0001* | −0.0833 |
| *Total horizontal coma vs angle $\lambda$* | | | |
| Group 1 ($n = 12$) | −0.1716 | 0.5751 | −0.0159 |
| Group 2 ($n = 15$) | −0.5699 | 0.0266 | −0.0099 |
| All eyes ($n = 27$) | −0.3618 | 0.0585 | −0.0108 |

et al., 2004).). An individual compensation of corneal spherical aberration was not found, as expected from the generic design of the intraocular lenses. Remarkably, an individual compensation (i.e. a significant correlation between internal and corneal spherical coefficients) had neither been found in young individuals. Furthermore, as previously reported in young eyes, we found a large compensation of horizontal coma in eyes with aspheric IOLs (87% as opposed to 51% in (Kelly et al., 2004).), both on average and in the individual eye correlations. It should be noted that our study, as well as previous studies did not include posterior corneal asphericity in the estimations of corneal aberrations. Dubbelman et al. 2007 showed a minor compensation of coma arising from the posterior cornea. Kelly et al. 2004 attributed part of the horizontal coma compensation to the eccentricity of the fovea, but they also hypothesized an active mechanism during development that would fine-tune the internal horizontal coma to match in magnitude (with opposite sign) that of the cornea. Our results do not favor this hypothesis, and rather support a passive mechanism, since we have found an even higher compensation with artificial generic IOLs of aspheric design. Simple computations using general eye models in a previous study (Kelly et al., 2004) seemed to suggest that the presence of a gradient index distribution in the lens would play a role in the compensation of horizontal coma. While certainly the gradient of index (GRIN) of the crystalline lens may have a major contribution to the spherical aberration of the eye, (and intraocular lens designs could incorporate this property), our data in patients with artificial lenses of constant refractive index demonstrate that compensation of horizontal coma is not determined by the presence of GRIN. Several authors (Artal et al., 2001; Kelly et al., 2004), have argued that compensation of horizontal coma may be achieved by fine-tuning of the crystalline lens position. While tilt and decentration of the lens do not appear to be major contributors to the compensation of horizontal coma, our data however support a compensatory role of lens misalignments, rather than an additional source of aberration (see Fig. 6). It is interesting
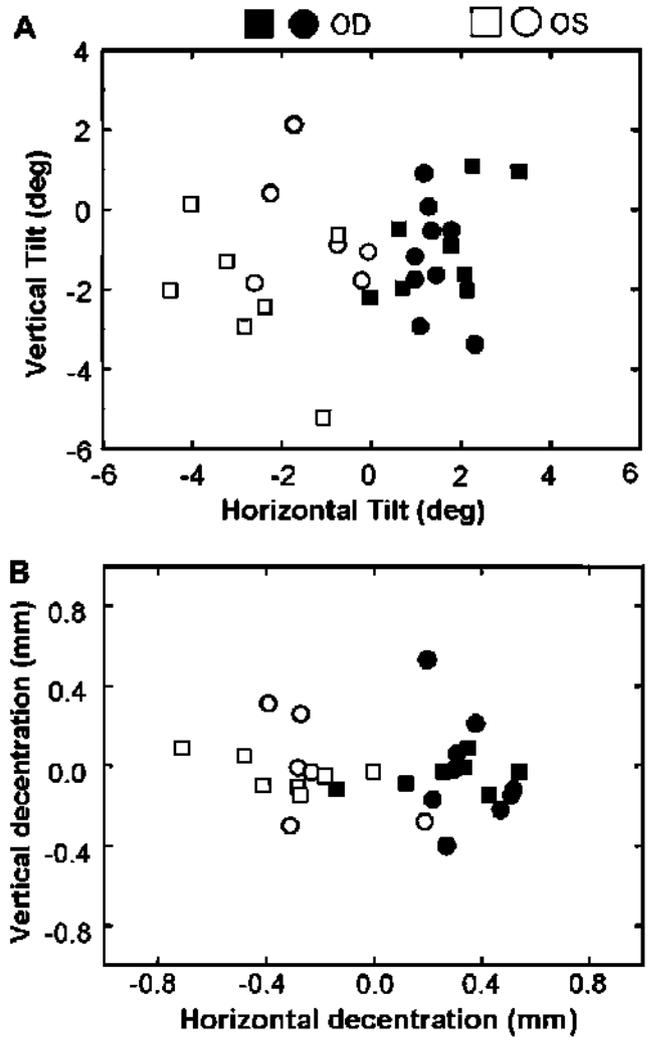


Fig. 5. Horizontal and vertical coordinates of (A) IOL tilt and (B) IOL decentration. Closed symbols stand for right eyes, and open symbols for left eyes. Circles stand for eyes from Group 1 and squares for eyes from Group 2. Signs convention for horizontal tilt (around the vertical axis) are: Positive, superior edge of the lens is closer to the cornea than the inferior edge, and vice versa for Negative. For vertical tilt (around the horizontal axis): Positive, nasal edge of the lens moves backward (for the right eye) or forward (for the left eye), and viceversa for Negative. Signs conventions for horizontal decentration are: For horizontal decentration: Positive, the lens is shifted toward the nasal (right eye) or temporal (left eye) direction and viceversa for Negative. For vertical decentration: Positive, the lens is shifted upward and viceversa for Negative.

that tilt and decentration appear to have a systematic bilateral symmetry and in the same direction than angle $\lambda$, in most eyes, even those implanted with intraocular lenses. We do not have preoperative data of crystalline lens tilt and decentration in these eyes, but a comparison with data in a young population from a previous study (Rosales & Marcos, 2006) suggests that surgery does not induce a significant increase in the magnitude of lens tilt and decentration and does not appear to change its orientation (perhaps preserved by the capsule). Whether this "beneficial" orientation of the lens was the result of an active process or a geometrical feature cannot be determined by our study,
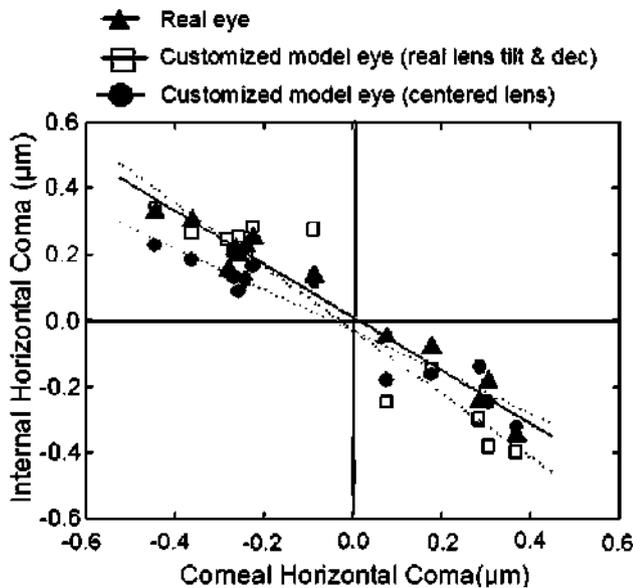
Fig. 6. Corneal versus internal horizontal coma for customized model eyes with IOLs (squares) aligned to the pupillary axis, misaligned according to the measured amounts of IOL tilt and decentration (diamonds) and for real aberration measurements (triangles). Linear correlations are highly statistical significant (coefficients of correlations are 0.96, 0.96 and 0.98, respectively. $p < 0.0001$). The lower slope (further from $-1$, indicative of lower compensation) correspond to eyes with centered IOLs ($-0.62$, as opposed to the eyes simulated with misaligned IOLs or real eyes, $-0.96$ and $-0.80$, respectively). Data correspond to eyes from Group 2.

but in any case the role of tilt and decentration of the lens in horizontal coma is small compared to that of foveal misalignment and surface geometry. Our study supports the hypothesis of a passive, geometry-driven mechanism for compensation of horizontal coma. In agreement with previous studies (Artal et al., 2006; Coletta et al., 2006), we found high correlation of corneal horizontal coma with the shift of the 1st Purkinje image from the pupil center (or angle $\lambda$). Unlike suggested by a previous model (Kelly et al., 2004), our customized eye model with IOLs shows similar results whether the 1st Purkinje shift is fully attributed to the eccentric fixation of the fovea or to a displacement of the pupil. Previous studies (Artal et al., 2006) conclude that the eye is a robust optical system, in the sense that eyes with different geometrical structure (such as hyperopes and myopes) exhibit similar optical performance (by compensation of spherical aberration and coma). We have not attempted to use refractive error as a variable in our study (although we have observed that longer eyes tended to have lower angle $\lambda$). However, our study also supports the robustness of the optical layout of the eye, in the sense that generic intraocular lenses with negative spherical aberration (but very different optical and geometrical structure than that of the crystalline lens) still are capable to produce an almost complete compensation of horizontal coma. This confirms the idea that the oblique incidence of rays that produces corneal horizontal coma, also generates coma in the lens, which for several designs (such as those of the

IOLs of this study, designed to produce negative spherical aberration) has opposite sign to that of the cornea. We have compared the amounts of absolute total horizontal coma in the eyes ($n = 27$) of this study ($0.067 \pm 0.049$ μm, for 5-mm pupil diameter) with a group of eyes ($n = 9$) of a previous study (Barbero et al., 2003), implanted with spherical IOLs (Acrysof, Alcon) using identical surgical technique, which showed significantly higher values of horizontal coma ($0.28 \pm 1.78$ μm). To our knowledge, no experimental study comparing optical performance of eyes with spherical and aspheric IOLs (Bellucci, Morselli, & Pucci, 2007; Marcos et al., 2005; Mester, Dillinger, & Anterist, 2003) have been able to find larger amounts of coma in eyes with aspheric IOLs compared to those with spherical IOLs, despite early predictions indicating that aspheric designs would be more susceptible to induce asymmetric aberrations in the presence of random tilt and decentrations (Atchison, 1989).

Our study also has implications for the design of aspheric IOL designs, which try to mimic the performance of the young crystalline lens, and particularly to compensate for off-axis coma (Tabernero, Piers, & Artal, 2007). We have found that two different designs (one with the asphericity in the anterior and the other with asphericity in the posterior surface of the lens) both produce similar compensation of horizontal coma for foveal fixation.

In order to investigate to which extent different designs could achieve a compensation of corneal horizontal coma, we evaluated computationally the optical performance of three different lenses minimizing defocus and spherical aberration (a meniscus, a biconvex lens with aspheric anterior surface and a biconvex lens with posterior aspheric surfaces) generated using analytical tools (Barbero & Marcos, 2007). Tests were performed on a customized pseudophakic eye model (Rosales & Marcos, 2007) for Eye #1 from Group 2. We found a compensation of spherical aberration with all three designs. However, horizontal coma increased by 20% for the meniscus lens, it decreased by 46% for the biconvex lens with aspheric anterior surface, and by 58% for the biconvex lens with aspheric posterior surface. This indicates that while not all, quite different designs can produce significant amounts of compensation. Also, we evaluated the behavior of a spherical and an aspheric IOL of the same optical power in the same model eye and found that simulated total horizontal coma was twice with the spherical than with the aspheric lens, in keeping with the experimental results. Finally, we simulated the off-axis optical performance using the customized model eye for Eye #1 from Group 2, with its actual IOL. We found that, while significant compensation of horizontal coma occurred over a few degrees of retinal eccentricities, there was a given angle ($-2$ deg for this eye) for which compensation was optimal (as opposed to 4 deg, which was the measured eccentricity for this eye). While maximum optical quality would be achieved if the fovea was located in the optimal position, compensation of horizontal coma in the eyes of the study is similar or even

better than in normal young eyes, indicating that significant compensations can be obtained with generic lenses not necessarily fine tuned to the foveal location.

## References

Applegate, R., Thibos, L., Bradley, A., Marcos, S., Roorda, A., Salmon, T., et al. (2000). Reference axis selection: Subcommittee Report of the OSA working group to establish standards for measurement and reporting of optical aberrations of the eye. *Journal of Refractive Surgery, 16,* 656–658.

Applegate, R. A., Donnelly, W. J., Marsack, J. D., Koenig, D. E., & Pesudovs, K. (2007). Three-dimensional relationship between high-order root-mean-square wavefront error, pupil diameter, and aging. *Journal of the Optical Society of America A-Optics Image Science and Vision, 24*(3), 578–587.

Applegate, R. A., & Howland, H. C. (1997). Refractive surgery, optical aberrations, and visual performance. *Journal of Refractive Surgery, 13,* 295–299.

Artal, P., Benito, A., & Tabernero, J. (2006). The human eye is an example of robust optical design. *Journal of Vision, 6*(1), 1–7.

Artal, P., Berrio, E., Guirao, A., & Piers, P. (2002). Contribution of the cornea and internal surfaces to the change of ocular aberrations with age. *Journal of the Optical Society of America A, 19,* 137–143.

Artal, P., & Guirao, A. (1998). Contributions of the cornea and the lens to the aberrations of the human eye. *Optics Letters, 23*(21), 1713–1715.

Artal, P., Guirao, A., Berrio, E., & Williams, D. R. (2001). Compensation of corneal aberrations by the internal optics in the human eye. *Journal of Vision, 1,* 1–8. doi:10.1167/1161.1161.116, http://journalofvision.org/1/1/1.

Atchison, D. A. (1989). Optical design of intraocular lenses .1. On-axis performance. Optometry and vision. *Science, 66*(8), 492–506.

Barbero, S., & Marcos, S. (2007). Analytical tools for customized design of monofocal intraocular lenses. *Optics Express, 15,* 8576–8591, http://www.opticsinfobase.org/abstract.cfm?URI=oe-15-14-8576.

Barbero, S., Marcos, S., & Merayo-Lloves, J. M. (2002). Total and corneal aberrations in an unilateral aphakic subject. *Journal of Cataract and Refractive Surgery, 28,* 1594–1600.

Barbero, S., Marcos, S., & Jimenez-Alfaro, I. (2003). Optical aberrations of intraocular lenses measured in vivo and in vitro. *Journal of the Optical Society of America A, 20,* 1841–1851.

Barry, J. C., Dunne, M., & Kirschkamp, T. (2001). Phakometric measurement of ocular surface radius of curvature and alignment: evaluation of method with physical model eyes. *Ophthalmic & Physiological Optics, 21,* 450–460.

Bellucci, R., Morselli, S., & Pucci, V. (2007). Spherical aberration and coma with an aspherical and a spherical intraocular lens in normal age-matched eyes. *Journal of Cataract and Refractive Surgery, 33*(2), 203–209.

Brunette, I., Bueno, J. M., Parent, M., Hamam, H., & Simonet, P. (2003). Monochromatic aberrations as a function of age, from childhood to advanced age. *Investigative Ophthalmology & Visual Science, 44*(12), 5438–5446.

Calver, R., Cox, M., & Elliott, D. (1999). Effect of aging on the monochromatic aberrations of the human eye. *Journal of Optical Society of America A, 16,* 2069–2078.

Coletta, N., Han, H., & Moskowitz, A. (2006). Internal compensation of lateral coma aberration: Relationship to refractive error: ARVO E-Abstract 1504. *Investigative Ophthalmology & Visual Science, 48.*

de Castro, A., Rosales, P., & Marcos, S. (2007). Tilt and decentration of intraocular lenses in vivo from Purkinje and Scheimpflug imaging—Validation study. *Journal of Cataract and Refractive Surgery, 33*(3), 418–429.

Dorronsoro, C., Barbero, S., Llorente, L., & Marcos, S. (2003). On-eye measurement of optical performance of rigid gas permeable contact lenses based on ocular and corneal aberrometry. *Optometry and Vision Science, 80,* 115–125.

Dubbelman, M., & Heijde, V. (2001). The shape of the aging human lens: Curvature, equivalent refractive index and the lens paradox. *Vision research, 41,* 1867–1877.

Dubbelman, M., Sicam, V. A. D. P., & van der Heijde, R. G. L. (2007). The contribution of the posterior surface to the coma aberration of the human cornea. *Journal of Vision, 7.* 1–8. doi:10.1167/7.7.10, http://journalofvision.org/7/7/10/.

Dubbelman, M., Sicarn, V., & Van der Heijde, G. L. (2006). The shape of the anterior and posterior surface of the aging human cornea. *Vision Research, 46*(6-7), 993–1001.

El Hage, S. G., & Berny, F. (1973). Contribution of the crystalline lens to the spherical aberratin of the eye. *Journal of the Optical Society of America A, 63*(2), 205–211.

García de la Cera, E., Rodriguez, G., & Marcos, S. (2006). Longitudinal changes of optical aberrations in normal and form-deprived myopic chick eyes. *Vision Research, 46*(4), 579–589.

Glasser, A., & Campbell, M. (1998). Presbyopia and the optical changes in the human crystalline lens with age. *Vision Research, 38*(2), 209–229.

Glasser, A., & Campbell, M. (1999). Biometric, optical and physical changes in the isolated human crystalline lens with age in relation to presbyopia. *Vision Research, 39,* 1991–2015.

Howland, H. C. (2005). Allometry and scaling of wave aberration of eyes. *Vision Research, 45*(9), 1091–1093.

Kelly, J. E., Mihashi, T., & Howland, H. C. (2004). Compensation of corneal horizontal/vertical astigmatism, lateral coma, and spherical aberration by internal optics of the eye. *Journal of Vision, 4*(4), 262–271.

Kisilak, M. L., Campbell, M. C. W., Hunter, J. J., Irving, E. L., & Huang, L. (2006). Aberrations of chick eyes during normal growth and lens induction of myopia. *Journal of Comparative Physiology A-Neuroethology Sensory Neural and Behavioral Physiology, 192*(8), 845–855.

Llorente, L., Barbero, S., Cano, D., Dorronsoro, C., & Marcos, S. (2004). Myopic versus hyperopic eyes: axial length, corneal shape and optical aberrations. *Journal of Vision, 4,* 288. http://journalofvision.org/4/4/5/.

Llorente, L., Diaz-Santana, L., Lara-Saucedo, D., & Marcos, S. (2003). Aberrations of the human eye in visible and near infrared illumination. *Optometry and Vision Science, 80.* 26–35.

Marcos, S., Barbero, B., Llorente, L., & Merayo-Lloves, J. (2001). Optical response to LASIK for myopia from total and corneal aberrations. *Investigative Ophthalmology and Visual Science, 42.* 3349–3356.

Marcos, S., Barbero, S., & Jiménez-Alfaro, I. (2005). Optical quality and depth-of-field of eyes implanted with spherical and aspheric intraocular lenses. *Journal of Refractive Surgery, 21.* 223–235.

Marcos, S., & Burns, S. A. (2000). On the symmetry between eyes of wavefront aberration and cone directionality. *Vision Research, 40,* 2437–2447.

Marcos, S., Díaz-Santana, L., Llorente, L., & Dainty, C. (2002). Ocular aberrations with ray tracing and Shack-Hartmann wavefront sensors: does polarization play a role? *Journal of the Optical Society of America A, 19,* 1063–1072.

Marcos, S., Rosales, P., Llorente, L., & Jimenez-Alfaro, I. (2007). Change in corneal aberrations after cataract surgery with 2 types of aspherical intraocular lenses. *Journal of Cataract and Refractive Surgery, 33*(2), 217–226.

Mclellan, J., Marcos, S., & Burns, S. (2001). Age-related changes in monochromatic wave aberrations in the human eye. *Investigative Ophthalmology and Visual Science*, 1390–1395.

Mester, U., Dillinger, P., & Anterist, N. (2003). Impact of a modified optic design on visual function: Clinical comparative study. *Journal of Cataract and Refractive Surgery*, *29*, 653–660.

Moreno-Barriuso, E., Marcos, S., Navarro, R., & Burns, S. A. (2001). Comparing laser ray tracing, spatially resolved refractometer and Hartmann-Shack sensor to measure the ocular wavefront aberration. *Optometry and Vision Science*, *78*, 152–156.

Phillips, P., Perez-Emmanuelli, J., Rosskothen, H. D., & Koester, C. J. (1988). Measurement of intraocular lens decentration and tilt in vivo. *Journal of Cataract and Refractive Surgery*, *14*, 129–135.

Rosales, P., Dubbelman, M., Marcos, S., & van der Heijde, R. (2006). Crystalline lens radii of curvature from Purkinje and Scheimpflug imaging. *Journal of Vision*, *6*, 1057–1067. doi:10.1167/6.10.5. http://journalofvision.org/6/10/5/.

Rosales, P., & Marcos, S. (2006). Phakometry and lens tilt and decentration using a custom-developed Purkinje imaging apparatus: validation and measurements. *Journal of the Optical Society of America A-Optics Image Science and Vision*, *23*(3), 509–520.

Rosales, P., & Marcos, S. (2007). Customized computer models of eyes with intraocular lenses. *Optics Express*, *15*(5), 2204–2218.

Rosales, P., Wendt, M., Marcos, S., & Glasser, A. (in press). Changes in the crystalline radii of curvature and lens tilt and decentration during dynamic accommodation in Rhesus Monkeys. *Journal of Vision*.

Sivak, J. G., & Kreuzer, R. O. (1983). Spherical aberration of the crystalline lens. *Vision Research*, *23*, 59–70.

Smith & al, E. (2001). The spherical aberration of the crystalline lens of the human eye. *Vision Research*, *15:41*(2), 235–243.

Smolek, M. K., Klyce, S. D., & Sarver, E. J. (2002). Inattention to nonsuperimposable midline symmetry causes wavefront analysis error. *Archives of Ophthalmology*, *120*(4), 439–447.

Tabernero, J., Piers, P., & Artal, P. (2007). Intraocular lens to correct corneal coma. *Optics Letters*, *32*(4), 406–408.

Tomlinson, A., Hemenger, R. P., & Garriott, R. (1993). Method for estimating the spheric aberration of the human crystalline lens in vivo. *Investigative Ophthalmology and Visual Science*, *34*(3), 621–629.